Int J Legal Med (1995) 108:157–161

TECHNICAL NOTE

I. Bajnóczky · L. Királyfalvi

A new approach to computer-aided comparison of skull and photograph

Received: 1 March 1995 / Accepted: 6 July 1995

Abstract A computer-based method developed for the purpose of checking the results of identification performed with the "traditional" method of video-superprojection (developed by Helmer and Grüner) is demonstrated; it does not require any special programs in addition to those necessary for digitising the video pictures. The method is suitable for filtering out "false-positive" cases. A great advantage is that the phase of computer evaluation can be separated from the job performed in the video studio, both in time and space. The process can be reconstructed, which means it can be checked. The results can be easily documented and interpreted for lay people.

Key words Video superprojection · Computer identification · Control of identification

Introduction

During identification procedures carried out by video superprojection, situations can arise where photographs of two or more persons show similar characteristics in the facial morphology. In addition, even small skull collections can include two skulls showing very similar constitutions. Computer-aided comparisons are then made to avoid false-positive identification and/or to verify the identity. Pesce-Delfino et al. (1986) have worked out a special program for the exclusion of false-positive results. Helmer et al. (1989a, b) have elaborated eight anthropometric points – out of a variety of such features – that are highly discriminative and therefore suitable for identification. Since the aforementioned approaches are mainly computer bases we have developed an additional procedure, which can be used as an independent check procedure during the process of identification. This approach does not require sophisticated software and can be carried out by a simple personal computer. The documentation is simple and easily understandable for lay people.

I. Bajnóczky (✉)
Institute of Legal Medicine, University Medical School, Pécs, Hungary

L. Királyfalvi
Central Research Laboratory, University Medical School, Pécs, Hungary

Materials and methods

The video superprojection utilises the methods developed by Helmer and Grüner (1977a, b).

The method developed here will be demonstrated on three items, i.e. one skull and two photographs. One of the photographs was of the person from whom the skull was derived (identical), while the other was of another person who was indistinguishable on the grounds of the skull in the procedure of superprojection. There were two photographs of this (non-identical) person: one taken from the norm frontalis and the other one from the norm lateralis.

Two approaches to identification were followed:

- We marked "afterwards" the measuring-points on the monitor, on the photograph and on the skull. These were digitised next to each other on the file.
- We marked the measuring points "before" directly on the photograph and the camera pictures were hereafter digitised "next to each other".

The whole experiment was thus based on six pairwise comparisons, i.e. skull with three photographs (3 pairs) by two methods (afterwards and before marking). From the four comparisons the following will be shown (Figs. 1–3) two afterwards comparisons with the non-identical person i.e. in two projections, each afterwards and before comparison with the identical person.

Equipment: video-camera (Sony Beta, SP PR 2000), cutting board (Sony DSF 5000 P), digitisation (Amiga 4000) using a picture-digitising program (Impact Vision 24 Frame Grabber, Image FX convertor program de Luxe Paint evocating program).

On the photographs, ca. 10 out of a variety of easily identifiable anatomical and/or anthropometrical points were selected and marked. According to Helmer et al. (1989a), we aimed at marking a minimum of 8 measuring points, but if there were more points available up to 12 points were marked. – The coordinate values of these points were recorded and expressed as pixel units (Tables 1, 2). From the raw data thus achieved, the final matrix was established by computer-aided processing (Table 3). Finally figures were produced demonstrating the anatomical and/or anthropometrical points from both items (skull/photograph) on 1 picture only (Figs. 1–3).

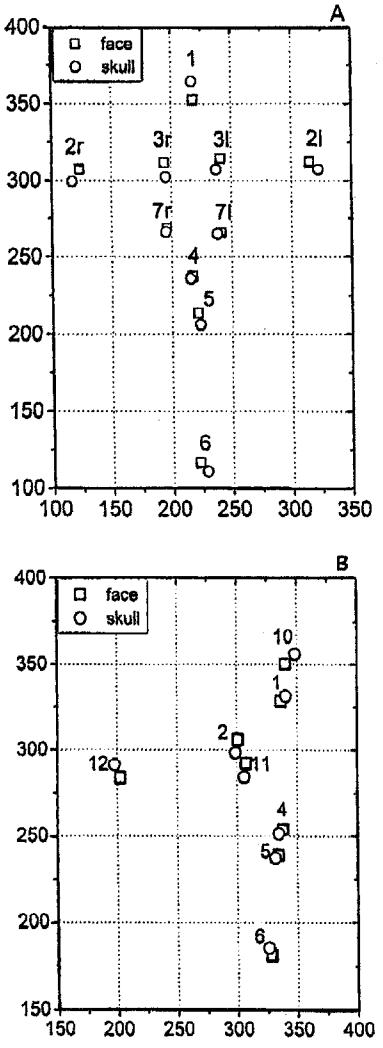

Fig. 1 Graphical representation of data from Tables 1–3. Comparisons of non-identical pairs (skull/photograph); two projections: **A** norm frontalis, **B** norm lateralis. Figures adjacent to measurement points according to Tables 1, 2. The differences between the pairs are according to the differences marked and processed and the directions reflect the anatomical positions

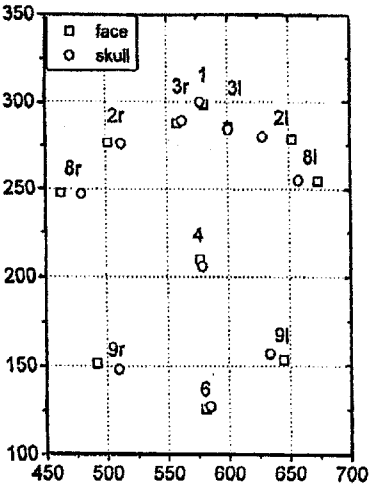

Fig. 2 Graphical representation of data evaluated and processed according to Tables 1, 2. Comparison of an identical pair (skull/photograph): "afterwards" assessment. Designation of measurement points 1–4 and 6 according to Table. Measurement points: *(8)* zygions; *(9)* gonions

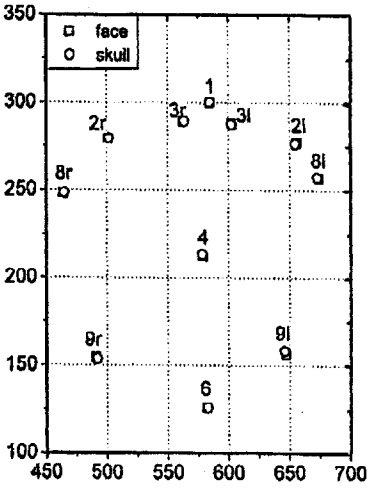

Fig. 3 Graphical representation of data evaluated and processed according to Tables 1, 2. Comparison of an identical pair (skull/photograph): "before" assessment. Designation of measurement points 1–4 and 6 according to Tables 1, 2. Measurement points: *(8)* zygions; *(9)* gonions

Processing and mathematical approaches

Suppose we have k frontal and m lateral points. Then the data matrix D consists of 2k + 2m coordinates measured for the face (column or variable named f) and their counterparts measured for the skull (variable named s), e.g.:

$$D = [f \quad s] = \begin{bmatrix} f_1 & s_1 \\ f_2 & s_s \\ f_3 & s_3 \\ f_4 & s_4 \end{bmatrix} = \begin{bmatrix} f_{11} & s_{11} \\ \dots & \dots \\ f_{1k} & s_{1k} \\ f_{21} & s_{21} \\ \dots & \dots \\ f_{2k} & s_{2k} \\ f_{31} & s_{31} \\ \dots & \dots \\ f_{3m} & s_{3m} \\ f_{41} & s_{41} \\ \dots & \dots \\ f_{4m} & s_{4m} \end{bmatrix} \begin{matrix} \} \text{ frontal, abscissae} \\ \\ \\ \} \text{ frontal, ordinates} \\ \\ \\ \} \text{ lateral, abscissae} \\ \\ \\ \} \text{ lateral, ordinates} \end{matrix}$$

(Note that if 1 + 1 photographs are used, then m = 0 or k = 0, and some partitions of the above matrix are missing. In the formulations below, we restrict ourself to the 2 + 2 case.)

Lacking the appropriate information, our models will assume that all data in D are independent and follow a normal distribution with the same variance. A part of this variance is σ^2, which is the square of the measurement error and is itself assumed to be the same with all the data.

We need f-s represented in a model that eliminates, as artificial effects, those effects from f-s that originate from the differences in choosing the systems of coordinates on the corresponding pictures. A simple model achieving this is a linear model that has a location parameter for each of the partitions of f - s. The error term of this model – say ε – can be looked upon as a reduced difference between f and s, which does not contain any systematic error resulting from shifting the origins. The expectation of ε is assumed to be zero, which means that the effects influencing ε (difference in the subjects and measurement errors) are random effects.

Table 1 Coordinate points of ten measurement points (norm frontalis) from a skull and a photograph

		Photo	Skull
1	Nasion (sellion)	219/341	545/357
2r	Eklokanthion (right)	308/318	642/317
2l	Eklokanthion (left)	129/315	450/312
3r	Endokanthion (right)	245/322	568/319
3l	Endokanthion (left)	193/321	521/316
4	Nasospinale (subnasale)	219/236	544/242
5	Prostion (labrale superius)	219/206	548/218
6	Gnathion	216/111	549/121
7r	Lateral point of the nose (right)	244/265	568/270
7l	Lateral point of the nose (left)	197/266	523/273

Table 2 Coordinate points of eight measurement points (norm lateralis) from a skull and a photograph

		Photo	Skull
10	Glabellare	332/344	618/346
1	Nasion (sellion)	332/325	624/324
2	Eklokanthion	302/314	578/302
11	Orbitale	309/300	585/288
4	Nasospinale (subnasale)	342/257	616/250
5	Prostion (labrale superius)	338/341	612/235
6	Gnathion	326/177	600/177
12	Porion	207/277	480/280

Interferences are based on the distance between the face and the skull, and this is measured by the square root of the variance of the components of ε, which is made up of two effects: the real differences in pattern or shape, and the measurement errors (errors in marking and recording the data points). Depending on the other information given, two basic types of inference can be considered.

In the first case, the photograph and the skull are known to have originated from one subject only. In this case,

ε cannot contain any effect arising from real pattern differences [1]

that is, the whole of our measure of distance arises from the measurement errors, and our model assumptions take the form:

the components of ε are independent and distributed according to $N(0,2\ \sigma^2)$ [2]

and $2\ \sigma^2$ can be estimated by $\hat{\varepsilon}'\hat{\varepsilon}/(2k + 2m - 4)$, where $\hat{\varepsilon}$ is the residual of the above model.

In the second case, subject identity is not known, and the measurement error cannot be estimated, but we use a presupposed value of σ (as part of the model assumptions). In this case, the assumption [1] is introduced as a null hypothesis (saying: " the subjects represented by the photograph and the skull are congruent in shape"). Under the null hypothesis, [2] is valid, and using this we conclude (refer to the so-called Cochran theorem in Seber 1966 and theorem 3.3.3. in Anderson 1958) that

$$\hat{\varepsilon}'\hat{\varepsilon}/(2\sigma^2)$$

has a χ^2 distribution of $2k + 2m - 4$ *df*. On this basis, the null hypothesis can be tested.

Table 3 Data matrix of the coordinates displayed in Tables 1 and 2 and values calculated

(1)	(2)	(3)	(4)	(5)	(6)
219	545	1	326	–0.9	218.1
308	642	1	334	7.1	315.1
129	450	1	321	–5.9	123.1
245	568	1	323	–3.9	241.1
193	521	1	328	1.1	194.1
219	548	1	329	2.1	221.1
219	544	1	325	–1.9	217.1
216	549	1	333	6.1	222.1
244	568	1	324	–2.9	241.1
197	523	1	326	–0.9	196.1
341	357	2	16	11.6	352.6
318	317	2	–1	–5.4	312.6
315	312	2	–3	–7.4	307.6
322	319	2	–3	–7.4	314.6
321	316	2	–5	–9.4	311.6
206	218	2	12	7.6	213.6
236	242	2	6	1.6	237.6
111	121	2	10	5.6	116.6
265	270	2	5	0.6	265.6
266	273	2	7	2.6	268.6
332	618	3	286	8.375	340.375
332	614	3	282	4.375	336.375
302	578	3	276	–1.625	300.375
309	585	3	276	–1.625	307.375
207	480	3	273	–4.625	202.375
342	616	3	274	–3.625	338.375
338	612	3	274	–3.625	334.375
326	606	3	280	2.375	328.375
344	346	4	2	6.125	350.125
325	324	4	–1	3.125	328.125
314	302	4	–12	–7.875	306.125
300	288	4	–12	–7.875	292.125
277	280	4	3	7.125	284.125
241	235	4	–6	–1.875	239.125
177	177	4	0	4.125	181.125

Data shown in the columns: *1* coordinates of the measuring points on the face; *2* coordinates of the measuring points on the skull; *3* particles (1 abscissae of the face and the skull in norm frontalis); (2 ordinates of the face and the skull in norm frontalis); (3 abscissae of the face and the skull in norm lateralis); (4 ordinates of the face and the skull in norm lateralis); *4* difference between the co-ordinate values of the skull and the face; *5* residual (difference between the co-ordinates of the skull shifted to the face and the co-ordinates of the face); *6* co-ordinates of the measuring points of the skull shifted to the face (co-ordinates of the points visible in Fig. 1)

Results and discussion

The distances between complying polygons, as shown in Figs. 1–3, are rather different in size. These size differ-

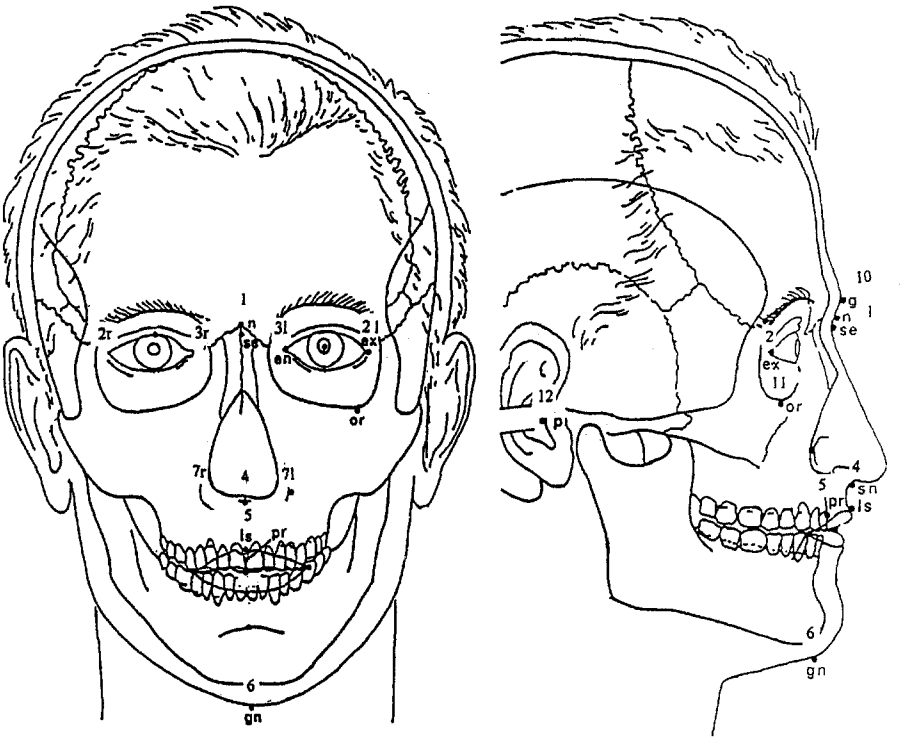

Fig. 4 Measurement points used in Tables 1, 2 and Figs. 1-3

ences can either originate from non-identity or from errors in the measurement technique. Such errors are mainly due either to imprecise positioning or to inaccuracies and/or imprecisions of the marking procedure. Figure 2 shows that the distances between the lateral polygons are approximately of the same magnitude and have the same magnitude on both sides. This would indicate that the error caused by imprecise rotation is rather small.

We tested the null hypothesis using two values for σ (with the program used for digitisation and the accompanying hardware, 1 mm is equivalent to 2.6 pixels). In case of a variance (measurement error) of 1 mm ($\sigma = 2.6$) the test is very significant ($P = 0.000024$), whole for 1.5 mm ($\sigma = 3.9$) it is not ($P = 0.409$). When a given case is evaluated it is crucial to know what value can be considered as measurement error. In the case of 1 mm, deviations cannot be explained by measurement faults. However, in the case of 1.5 mm such errors can prevent the detection of existing deviations (further conclusions could be possible if a broader information of data from a larger population survey were available). It is therefore absolutely necessary to determine the tolerance limit of the measurement error. Otherwise – in addition to producing significant errors – a "false exclusion" is also a possibility, even in a case of identical skull-photo pairs.

From Fig. 2 the influence of the marking procedure in combination with the 3-dimensional shape and the dimension differences between skull and photographs can be derived. The latter differences are mainly due to the soft tissue, while the first type of difference is due to the photographic process, which results on the one hand in a roughly equivalent representaiton of the approximately plane middle part of the face, and on the other in a much greater distortion of the lateral parts. These features would provide a logical explanation for the extent of differences between "identical" points and also their horizontal deviation. This type of systematic deviation was markedly expressed in the comparisons derived from the "afterwards" method.

The "before" marking procedure was not associated with the aforementioned type of deviation. We ascribe this to the methods of assessing the measurement points. The afterwards method is impaired by the more diffuse image of the picture on the monitor and also by the methodology of assessment with a mouse. These two factors seem to be decisive, especially when lateral points are to be considered. Especially here, because of the influence of the soft tissue and the photographic distortion, influences of small errors obviously become more crucial.

The method described has the advantages of being easily reproducible and easily controlled by other experts. The result can be documented and interpreted in a way that is also comprehensible to lay people. Nonetheless, it should be used only in combination with classic video-superprojection and could be regarded as an independent check.

References

Anderson TW (1958) An introduction to multivariate statistical analysis. Wiley, New York

Helmer R, Grüner O (1977a) Vereinfachte Schädelidentifizierung nach dem Superprojektionsverfahren mit Hilfe einer Video-Anlage. Z Rechtsmed 80: 183–187

Helmer R, Grüner O (1977b) Schädelidentifizierung durch Superprojektion nach dem Verfahren der elektrischen Bildmischung, modifiziert zum Trickbild-Differenz-Verfahren. Z Rechtsmed 80:189–190

Helmer R, Schimmler J, Rieger J (1989a) On the conclusiveness of skull identification via the video superimposition technique. Can Soc Forensic Sci J 22:177–194

Helmer R, Schimmler J, Rieger J (1989b) Zum Beweiswert der Schädelidentifizierung mit Hilfe der Video-Bildmischtechnik unter Berücksichtigung der kraniometrischen Individualität menschlicher Schädel. Z Rechtsmed 102:451–459

Pesce-Delfino V, Colonna M, Vacca E, Potente F, Introna F (1986) Computer-aided skull/face superimposition. Am J Forensic Med Pathol 7:201–212

Seber GAF (1966) The linear hypothesis: a general theory. Griffin, London